

Radius dependence of Aharonov-Casher spin interference in InGaAs ring arrays

Fumiya Nagasawa¹, Jun Takagi¹, Yoji Kunihashi¹, Makoto Kohda^{1,2}, and Junsaku Nitta¹

¹Graduate School of Engineering, Tohoku University, Sendai 980-8579, Japan

²PRESTO-Japan Science and Technology Agency, Saitama 331-0012, Japan

E-mail: b1tm5327@s.tohoku.ac.jp

1. Introduction

All-electrical manipulation and detection of spins in solid state devices have significant importance for future spintronics. Our proposed spin-interference device [1], which consists of a ring-shaped two-dimensional electron gas and a top-gate electrode, has preferable characteristics in such points: (i) tunable spin orientations by a gate voltage through Rashba spin-orbit interaction (SOI); (ii) detectable spin phase differences as an oscillatory behavior in a resistance; (iii) needless to polarize spins because a spin interference occurs to each and every spin with itself. By employing the spin-interference device, T. Bergsten *et al.* have observed an Aharonov-Casher (AC) spin interference effect as resistance oscillations depending on the gate voltage [2]. The oscillatory behavior in the resistance is induced by differences in spin-precession angles between wave functions propagating clockwise and counterclockwise directions of loops. In this simple picture, one can readily imagine that different lengths of propagation paths for wave functions results in distinct precession angles. Hence, the AC effect will depend on a ring radius. So far, however, the radius dependence of the AC effect has not been observed clearly. In this study, we focus on the AC effect in ring arrays with various radii.

2. Experiment and Discussion

Two samples which differ in the ring radius r and the number of rings were fabricated from an InAlAs / InGaAs based two-dimensional electron gas by electron beam lithography and reactive-ion etching. A typical geometry of samples is shown in Fig. 1. A smaller radius sample, $r = 620$ nm, and another one with $r = 860$ nm, have 40×40 and 50×50 arrays of rings, respectively. Both arrays are covered with an Al_2O_3 insulator with the same thickness of 200 nm, deposited by atomic layer deposition, and a Au top-gate electrode in order to control the Rashba SOI by the gate voltage.

Note that a gate field tunes not only the strength of the Rashba SOI, but a carrier density, i.e., an electron wave length. To observe the AC spin interference effect, one has to eliminate an interference contribution from the orbital part of wave functions. For this purpose, by applying a perpendicular magnetic field to ring arrays, a time-reversal Al'tshuler-

Aronov-Spivak (AAS) effect has been measured at static gate voltages.

The magnetoresistance curve of the $r = 860$ nm sample with the gate voltage $V_g = -1.4$ V at $T = 1.7$ K is shown in the Fig. 2(a). A parabolic component of the curve results from the localization effect, and oscillations, which are suppressed at higher magnetic fields, are the AAS effect

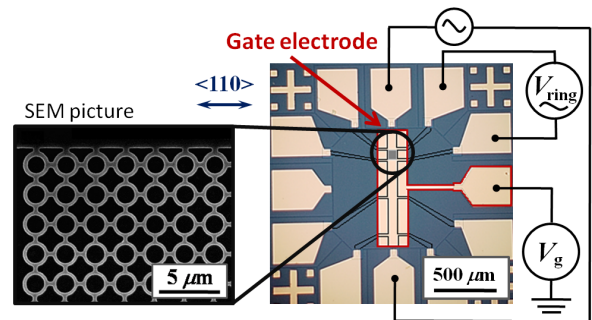


FIG. 1. Top-view image of a sample and SEM picture of a ring array. The gate electrode covers whole area of the ring array and a Hall bar. Fabricated two samples are different in radius and the number of rings: one is the 40×40 array of 620 nm radius rings, another is the 50×50 array of 860 nm radius rings.

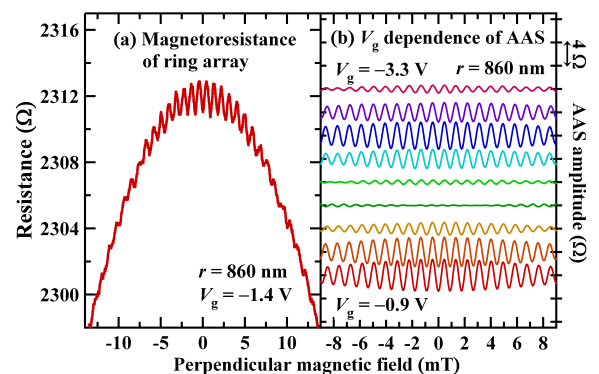


FIG. 2. (a) Magnetoresistance curve for $r = 860$ nm sample. The curve has been measured at the static gate voltage $V_g = -1.4$ V, and the temperature of 1.7 K. (b) Gate voltage dependence of extracted AAS oscillations. The AAS oscillations are plotted every 0.3 V of the gate voltage V_g from -3.3 V to -0.9 V. Amplitudes of the AAS effect are clearly modulated by the gate voltage.

($h/2e$ periods in the magnetic flux). Similar magnetoresistance curves have been obtained at each gate voltage. In the next step, AAS oscillations are picked up from the curves. As one can see in Fig. 2(b), AAS amplitudes are modulated by the gate voltage. Notice that without the spin interference, AAS oscillations have a peak at zero magnetic field in magnetoresistance curves, however, Fig. 2(b) shows dips at the magnetic field of 0 T in the oscillations. This phenomenon is attributed to the spin interference effect.

To observe the pure spin-interference effect, i.e., the AC effect, the AAS amplitudes are plotted as a function of gate voltage. Figures 3(a) and 3(b) show AC oscillations in 620 nm and 860 nm radius samples, respectively. Both figures indicate that the AC oscillations have negative component in its amplitude. The component can be attributed to the weak antilocalization effect.

As one can read off from Figs. 3(a) and 3(b), the gate voltage period of AC oscillations, ΔV_g , is confirmed to be $\Delta V_g = 2.2$ V for smaller radius sample, and $\Delta V_g = 1.8$ V for larger one. In our system, a precession angle θ is given by [3]

$$\theta = \frac{2\alpha m^* L}{\hbar^2}, \quad (1)$$

where α is the strength of the Rashba SOI, L is the travelled distance. The experimental result can be qualitatively explained by the equation above. The larger radius meaning the longer L results in larger precession angle θ . Therefore the larger radius sample has the larger phase change.

To clarify the radius dependence of the AC period in more detail, calculated results are plotted in Figs. 3(a) and 3(b) as dashed lines. For the interference between time-reversal

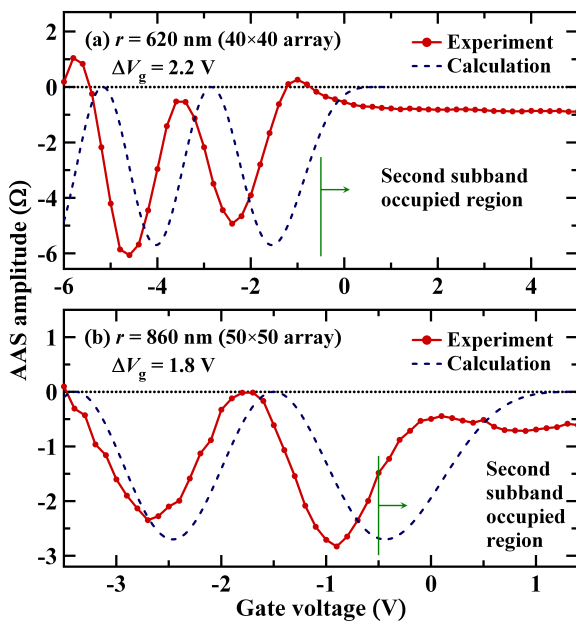


FIG. 3. AC effect in (a) 40×40 array, 620 nm in radius, (b) 50×50 array, 860 nm. Both measurements were performed at 1.7 K.

paths, amplitudes of AC oscillations are expressed as [4]

$$\frac{\delta R_{\alpha \neq 0}}{\delta R_{\alpha = 0}} = \cos \left[2\pi \sqrt{1 + \left(\frac{2m^* \alpha}{\hbar^2} r \right)^2} \right], \quad (2)$$

where $\delta R_{\alpha \neq 0}$ and $\delta R_{\alpha = 0}$ are AC amplitudes with and without the Rashba SOI. The calculated periods of the AC interference are consistent with the experimental results. Here the gate voltage dependence of α was obtained from the weak antilocalization. Note that phases are slightly different between experimental results and calculated ones. The phase discrepancy might be attributed to the existence of the finite Dresselhaus SOI which is expected in the III-V compound semiconductors. A phase shift in the AC oscillation is predicted in the presence of the Dresselhaus SOI [5].

In Figs. 3(a) and 3(b), there is another intriguing phenomenon. That is, for both samples, AC oscillations are suppressed at gate voltages above -0.5 V. From the analysis of Shubnikov-de Haas oscillations, it has been revealed that in the region $V_g > -0.5$ V, the second subband is occupied. In the presence of two subbands, there two Rashba parameters α_1 and α_2 exist. Considering Eq. (1), the suppression mechanism can be ascribed to the ensemble averaging in the precession angle θ due to the presence of different values of α .

3. Conclusion

The time-reversal AC effect has been investigated in two samples with two different radii. The gate voltage period of the AC oscillations has been confirmed to be $\Delta V_g = 2.2$ V for smaller radius sample and $\Delta V_g = 1.8$ V for larger radius sample. As numerical calculations have quantitatively reproduced those periods, we have successfully observed radius dependence of the AC effect. A slight phase shift from experimental results can be attributed to the existence of the Dresselhaus spin-orbit interaction. Also, suppression of the AC oscillations has been observed in the second subband occupied region. The suppression of the spin interference is induced by the inter-subband scattering.

References

- [1] J. Nitta, F. E. Meijer, and H. Takayanagi, *Appl. Phys. Lett.* **75**, 695 (1999).
- [2] T. Bergsten, T. Kobayashi, Y. Sekine, and J. Nitta, *Phys. Rev. Lett.* **97**, 196803 (2006).
- [3] S. Datta and B. Das, *Appl. Phys. Lett.* **56**, 665 (1990).
- [4] D. Frustaglia and K. Richter, *Phys. Rev. B* **69**, 235310 (2004).
- [5] M. J. van Veenhuizen, T. Koga, and J. Nitta, *Phys. Rev. B* **73**, 235315 (2006).